Novel Applications of MOEMS Display and Imaging

Ming C. Wu
Department of Electrical Engineering and Computer Sciences
University of California, Berkeley, CA 94720

ABSTRACT

Significant progresses have been made in MOEMS for display, imaging, telecommunication, and bioinstrumentation applications. This talk will first provide an overview of the recent advances in micromirror technologies. Then it will discuss three novel applications using MEMS micromirrors. First, a large port count wavelength-selective switch using a one-dimensional array of two-axis analog micromirrors will be described. Then the fabrication and packaging of two-axis micromirrors for in vivo endoscopic optical coherence tomography (OCT) imaging will be presented. Finally a new "optoelectronic tweezers" for manipulating microparticles and biological cells using direct images of MOEMS spatial light modulators will be described.

Keywords: MOEMS, wavelength-selective switches, WDM, endoscopic imaging, optoelectronic tweezers, optical manipulation

1. INTRODUCTION

There has been an explosive growth of the micro-opto-electro-mechanical-system (MOEMS) technology in the past several years, fueled primarily by the boom in telecom market. A wide variety of MOEMS devices and systems have been developed. Though not all the companies or operations started during that time survived the market downturn, remarkable progresses have been made in the MOEMS technologies, particularly in the manufacturing, packaging, and reliability of MEMS devices. In this paper, we will summarize the advances in three applications: wavelength-selective switches for telecommunication networks; MEMS endoscopic imaging devices; and a direct image-driven optoelectronic tweezers for parallel manipulation of microparticles.

2. MICROMIRROR ARRAY FOR TELECOMMUNICATION APPLICATIONS

During the telecom boom, many companies focused on the development of large switching fabrics. They are generally called three-dimensional (3-D) MEMS switches because the optical beams are steered in free-space across two-dimensional array of output collimators. Optical switches with port count ranges from 64x64 to 1000x1000 have been demonstrated [1-18]. Though market expectation for these switches has not been realized, remarkable progresses have been made in the manufacturing of two-axis MEMS mirrors. Sophisticated control and monitoring algorithms have been developed to precisely control and maintain the pointing angles of the mirrors. Smaller optical switches using two-dimensional array of digital switching elements, generally called 2-D MEMS switches, have also been extensively developed [20-29]. The 2-D switches are more compact, usually can be monolithically integrated on a single chip, and consume much less power compared with 3-D switches. Their port count is limited to below ~ 32x32 by optical diffraction. Commercial 2-D switches, with port count of 16x16 for single-chip switches and 32x32 for cascaded switches, have been realized using moving mirrors [27]. More significantly, they have passed the stringent Telecordia reliability test.

Recently, there has been increasing attention on smaller but more versatile wavelength-selective switches (WSS). They stem from dynamically reconfigurable wavelength add-drop multiplexer (WADM) [30], but their output port count is greater than one. They are generally referred to as 1xN WSS, where N is the output port count. The various wavelengths in the wavelength-division-multiplexed (WDM) optical signals are first demultiplexed by a free-space

Micromachining and Microfabrication Process Technology X,
edited by Mary-Ann Maher, Harold D. Stewart, Proc. of SPIE Vol. 5715
(SPIE, Bellingham, WA, 2005) · 0277-786X/05/$15 · doi: 10.1117/12.608014

grating. The diffracted beams are focused onto a 1-D array of analog micromirrors, which steer the individual wavelengths to their output ports independently. The output wavelengths are then re-multiplexed by the same grating and collected by separate output fiber collimators.

An analog micromirror array with a large continuous scan angle is the key enabling component. Each individual wavelength can be independently directed to any of the N output fibers, depending on the angle of the corresponding micromirror. In addition, high fill factor is desired to minimize the gaps between WDM channels. The mirror size is usually several times larger than the focused spot size of the Gaussian beam to attain a flat spectral shape for the passband ("flat-top" spectral response). Hah et al. has developed a low-voltage analog micromirror array for 1xN wavelength-selective switches [31,32]. They are fabricated using the five-layer surface micromachining process offered by Sandia National Lab's SUMMiT-V foundry service [33]. Actuated by the powerful vertical comb-drives, the mirrors have extremely low operating voltages. The actuator is also free from pull-in instability which is characteristic of parallel-plate electrostatic actuators, further extending the rotation angle. A maximum mechanical scan angle of ± 6° is achieved at 6V actuation voltage for 0.5-μm gap spacing. The actuators and the torsion springs are completely covered by the mirror so that high fill factor is achieved along the array direction. The resonant frequency is greather than 3 kHz.

Marom et al. were the first to demonstrate the system-level performance of the architecture of 1xN WSS [34]. Their 1x4 wavelength-selective switch supports 128 WDM channels at 50 GHz spacing. A resolution lens of 10-cm focal length and an 1100-gr/mm grating provide the necessary spatial dispersion. Using a micromirror with ±8° at 115 V made on an silicon-on-insulator (SOI) wafer, a flat-top spectral response and an optical insertion loss of 3 to 5 dB were obtained. Their modified system was reported later [35] and new mirrors have been developed to match the requirement of the improved system [36,37]. This modified system utilizes anamorphic compression on the light beam to reduce the system size. It also supports a 10-dB dynamic equalization range. System performance of other 1x4 WSS's has also been reported by Huang et al. [38] and Ducellier et al. [39]. Corning IntelliSense Corp. also developed MEMS scanner array for this particular application [40].

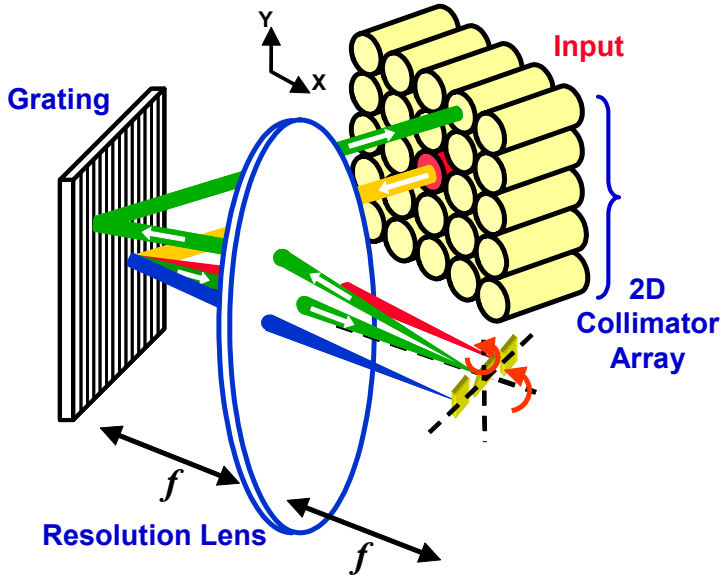

Fig. 1. Schematic of 1xN^2 wavelength-selective switches (WSS). The port count of the WSS is increased from N to N^2, where N is the maximum linear port count allowed by optical diffraction. [41]

The maximum port count of the reported 1xN WSS is 4, limited by optical diffraction. A larger port count (N > 10) is desirable in telecommunication. UCLA has developed a new WSS architecture, called 1xN^2 WSS [41,42]. It uses a 2-D

array of fiber collimators in conjunction with a 1-D array of 2-axis analog micromirror array. This expands the port count from N to N^2, where N is the maximum linear port count allowed by optical diffraction. Figure 1 shows the schematic of the $1xN^2$ WSS. A critical enabling element for such switches is a two-axis analog micromirror array with high fill factor along the array direction and large scan ranges in both axes. UCLA has reported a two-axis analog micromirror array with 96% fill factor, achieved by using novel bi-directional cross-bar torsion springs underneath the mirror [43]. A quadrant electrode with terrace electrode actuates the mirror. The terrace electrodes reduce the actuation voltage by about 25 to 34%. Figure 2 shows the scanning electron micrographs (SEM) of the two-axis micromirror. The devices are fabricated using the SUMMiT-V surface micromachining process. As mentioned previously, it has five polysilicon layers, including one nonreleasable ground layer (mmpoly0) and four structural layers (mmpoly1 to mmpoly4). The terraced electrodes are made of the bottom four polysilicon layers (mmpoly0 to mmpoly3), whereas the top polysilicon layer (mmpoly4) is designated for the mirror. In the SEM picture, half of the mirror is intentionally removed to reveal the underlying structures. Large mechanical scan angles (±4.4° and ±3.4°) have been achieved. The resonant frequency of the mirror is greater than 20.7 kHz. A 1x14 WSS (3x5 collimator array) was also constructed using the two-axis mirror array. The channel spacing is 50 GHz, and the fiber-to-fiber insertion is 8.2 dB.

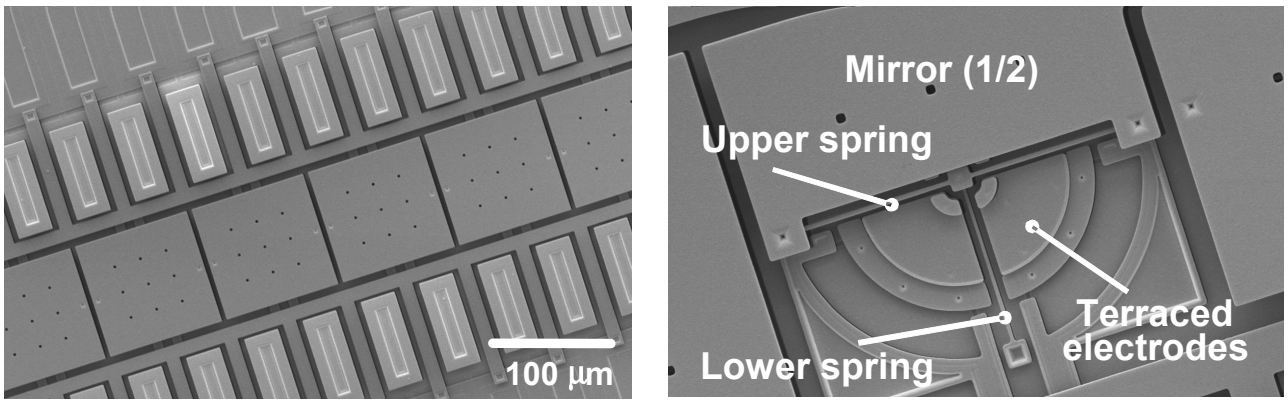

(a) (b)

Fig. 2. (a) SEM of the 2-axis analog micromirror array. (b) Close-up of the 2-axis micromirror with half of the mirror removed to reveal the bi-directional cross-bar torsion springs and the quadrant terrace electrodes. [43]

To fully exploit the capacity of the $1xN^2$ WSS, Tsai et al. have developed a novel gimbal-less lever-driven two-axis analog micromirror array with large scan angles (+/- 6.7° for both axes) and high fill factor (98%) [44]. The actuation voltage is 75V. The scanner is actuated by four motion-amplifying levers. Compact compliant 2-DOF mirror joints are employed. They transform the lever-enhanced lifts into two-axis tilt. The devices are again fabricated using SUMMiT-V surface micromachining process. It consists of three serpentine springs in a T-configuration, permitting the mirror to tilt around both axes. The size of the mirror is 196x196 μm^2, on a pitch of 200 μm. The measured mechanical resonant frequency is 5.9 kHz. A 1x32 WWS has been implemented using this two-axis scanner array. The channel spacing is 100 GHz and the insertion loss is 3.72 dB [45]. To our knowledge, this is the highest port count ever reported for WSS.

3. MEMS ENDOSCOPIC IMAGING DEVICES

Endoscopic imaging with cellular resolution is an area of intense interest. MEMS is a key enabling technology for incorporating miniature beamsteering components in a package compatible with standard endoscopic ports. There are tow main approaches for three-dimensional (3-D) *in vivo* imaging: confocal microscopes and optical coherence tomography. The discussion in this paper will focus on endoscopic optical coherence tomography (EOCT). EOCT is an emerging technology for high-resolution endoscopic imaging of biological tissues *in vivo* and in real time [46]. EOCT can distinguish architectural layers *in vivo* and can differentiate normal from tumor lesions within the human

gastrointestinal tract. A need for compact, robust scanning devices for endoscopic applications has fueled the development of MEMS scanning mirrors for confocal imaging [47-50] and for optical coherence tomography [51-53]. Demonstrations of MEMS scanning OCT endoscopes to date, however, have been limited to single-axis scanning.

Researchers at MIT and UCLA have developed the first two-dimensional endoscopic MEMS scanner for high resolution optical coherence tomography [53]. The 2-D scanner with angular vertical comb actuators (AVC) is fabricated by using surface and bulk micromachining techniques [54]. The AVC actuators provide high-angle scanning at low applied voltage [55,56]. The combination of both fabrication techniques enable high actuation force, large flat micromirrors, flexible electrical interconnect, and tightly-controlled spring constants, as shown schematically in Fig. 3. A single-crystalline silicon (SCS) micromirror is suspended inside a gimbal frame by a pair of polysilicon torsion springs. The gimbal frame is supported by two pairs of polysilicon torsion springs. The four electrically isolated torsion beams also provide three independent voltages to inner gimbals and mirrors. The SEM of the finished device is shown in Fig. 4. The torsion spring is 400 µm long, 10 µm wide, and 4.5 µm thick. The scanner has 8 comb banks with 10 movable fingers each. The finger is 5 µm wide, 150 µm long, and 35 µm thick. The gap spacing between comb fingers is 4 µm. The mirror is 1000 µm in diameter and 35 µm thick. The AVC banks are fabricated on SCS. The movable and fixed comb banks are completely self-aligned.

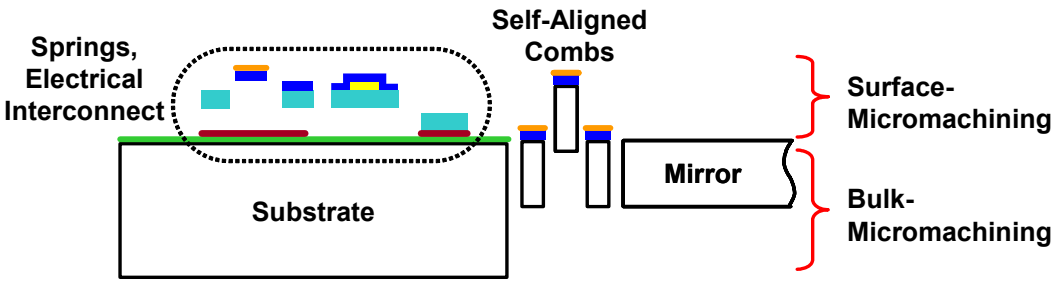

Fig. 3. Schematic cross-section of the hybrid surface-/bulk-micromachined 2-D MEMS scanner. The surface-micromachined structures provide the compliant, controllable mechanical springs and electrically isolated electrical interconnect, while the bulk-micromachined structures provide flat micromirrors and the power angular vertical combdrive (AVC) actuators.

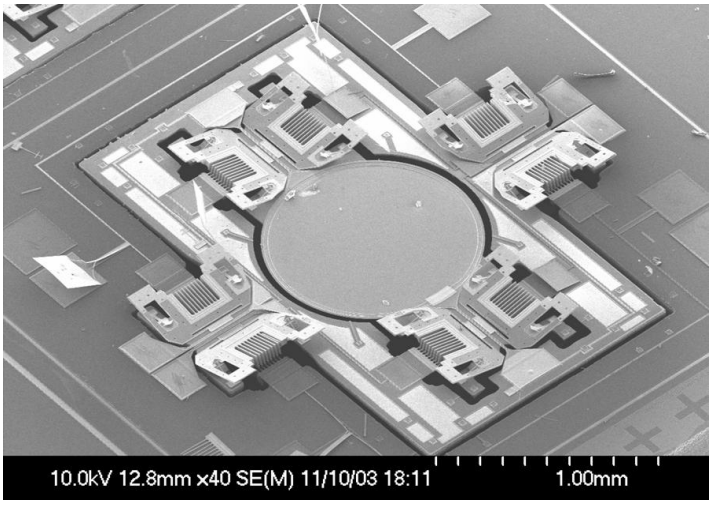

Fig. 4. SEM of the 2-D MEMS scanner with AVC actuators [53].

Figure 5 shows the schematic of the fiber coupled MEMS scanning endoscope. The endoscope head is 5-mm in

diameter and 2.5-cm long, which is compatible with standard endoscope ports. The compact aluminum housing can be machined at low cost and allows precise adjustment of optical alignment using tiny set screws. The optics consists of a graded-index fiber collimator followed by an anti-reflection coated achromatic focusing lens producing a beam diameter (2w) of ~ 13 μm [53]. The 2-D MEMS scanner is mounted at 45° and directs the beam orthogonal to the endoscope axis in a side-scanning configuration similar to those typically used for endoscopic OCT procedures. Post-objective scanning eliminates off-axis optical aberration encountered with pre-objective scanning. The large 1-mm diameter mirror allows high-numerical-aperture focusing. A sawtooth drive waveform of 30-70 volts was used to scan the mirror at frequencies up to 20 Hz for imaging. A modelocked Cr^{4+}: Forsterite laser centered at 1250 nm with ~ 180-nm bandwidth is used to achieve 5-μm axial resolutions. *In vivo* images of the human dermis and nail fold region are acquired at up to 20 frames per second.

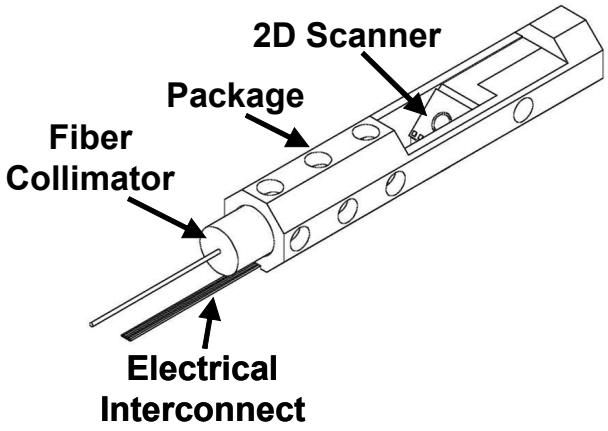

Fig. 5. Schematic of the MEMS EOCT head [53].

4. OPTOELECTRONIC TWEEZERS FOR PARALLEL MANIPULATIONS

Cellular-scale manipulation is an important tool in biological research. Technologies that have demonstrated the capability for such microscopic manipulation include optical tweezers and dielectrophoresis [57,58]. While optical tweezers affords very fine control of microparticles, it suffers from high optical power requirements. Dielectrophoresis has been demonstrated to trap particles as small as 14 nm [59]. However, dielectrophoresis requires a static pattern of electrodes, and is not easily reconfigurable.

We have demonstrated another method of manipulating micrometer-scale objects: optically-induced dielectrophoresis, or optoelectronic tweezers [60]. Using a laser to induce dielectrophoretic forces, we have demonstrated controlled movement of 25-μm latex particles, and *E. coli* bacteria [60,61]. This technique allows the use of very low optical power levels, enabling us to perform particle manipulation with an incoherent light source [62,63]. The use of a spatial light modulator in our optical system also allows us to dynamically reconfigure particle traps, providing us with increased versatility in particle manipulation over conventional dielectrophoresis. Dynamic *array manipulation* of microparticles using optoelectronic tweezers was demonstrated for the first time. We demonstrated the self-organization of particles into an array, and the formation of single-particle arrays, with the capability to individually address each particle.

The optical power required to induce DEP forces in OET is much lower than that of optical tweezers, as the light energy does not directly trap the particles. Early experiments using OET showed movement of 25 μm particles at 4.5 μm/sec with an optical power of 1 μW, corresponding to an incident power density of 440 mW/cm^2 [60]. In comparison, a 1 μm diameter optical tweezers trap, at a minimum trapping power of 1 mW, has an optical power density of 32 kW/cm^2. The low optical power requirements of OET offer many advantages in the system design.

Inexpensive incoherent light sources can be employed instead of lasers to provide the illumination necessary for OET [62,63]. In addition, we can produce light patterns by imaging rather than scanning techniques. Furthermore, with no need to focus all optical energy, we can use a simple spatial light modulator to pattern images, rather than the holographic techniques employed by optical tweezers arrays [64]. In our experiments, we used the digital micromirror device (DMD) [65] in a light projector to image the virtual electrodes.

The optoelectronic tweezers device is formed by evaporating a 10-nm-thick aluminum film onto a glass substrate for electrical contact. A 1-μm-thick undoped amorphous silicon (a-Si) photoconductive layer is then deposited by plasma-enhanced chemical vapor deposition. To protect the photoconductive film, a 20-nm-thick silicon nitride layer is deposited over the a-Si. The liquid buffer layer containing the particles of interest is sandwiched between this photoconductive device and indium-tin-oxide (ITO) glass (Fig. 6). An applied ac bias across the ITO and a-Si produces the electric field.

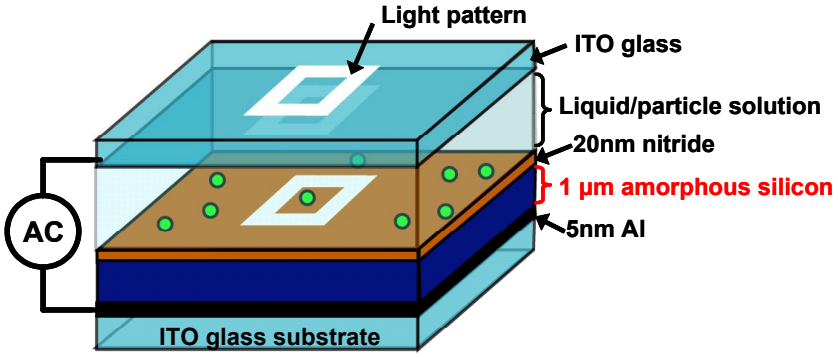

Fig. 6. Schematic structure of the optoelectronic tweezers (OET). The liquid containing the microparticles of interest is sandwiched between a top ITO glass and a bottom photoconductive electrode [60].

A DMD-based projector (InFocus LP335) is used to display images drawn on a PC, via Microsoft PowerPoint software. The projector provides both the optical source (a 120W, 1000-ANSI lumen high-pressure mercury lamp) and the DMD-to-PC interface. The output of the projector is collected, collimated, and directed into an Olympus MSPlan10 10X objective lens (NA = 0.30), projecting an image onto the OET device. The power at the projector output was measured to be approximately 600 mW. Approximately 7% of this power is collected by the objective lens and focused onto the OET device. Therefore, the power of the light incident on the OET is 42 mW, corresponding to an intensity of 12 W/cm^2.

The buffer solution consists of deionized water and KCL salt, mixed to obtain a conductivity of 10 mS/m. Polystyrene microspheres are mixed into the buffer solution, and sandwiched into the OET device. Observation of the particles under test is done via a Nikon TE2000U inverted microscope. A CCD camera attached to the observation port of the microscope recorded images and video of our experiments. A schematic of the optical setup is shown in Fig. 7. To produce the electric field necessary for DEP, an ac voltage of 10Vpp at 100 kHz was applied across the top ITO surface and the bottom photoconductive surface of the OET device.

Figure 8 shows an example of parallel manipulation of individual 45-μm polystyrene particles. Each randomly positioned particle is first contained within a square trap. This is performed by drawing a rectangle around each particle. The multiple traps can then be positioned to form an array of individually addressable cells. Using this technique, we are able to form a 4x5 array of single particle traps (Fig. 8). The capturing and arranging process can potentially be automated by combining OET with a vision system. Biological applications of such an array include studies on single-cell behavior and interaction.

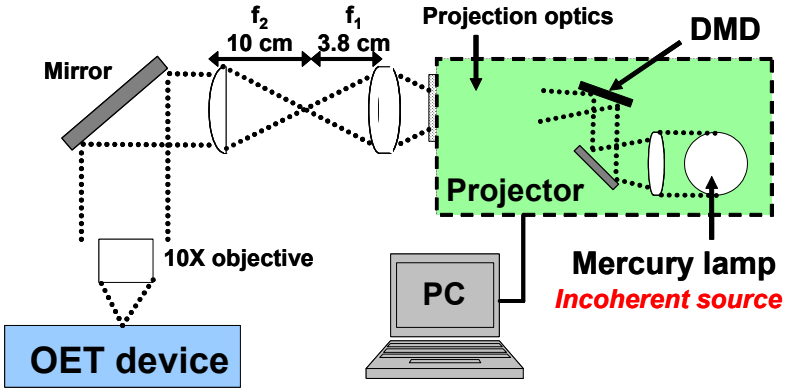

Fig. 7. Schematic diagram illustrating the setup for optoelectronic tweezers [63].

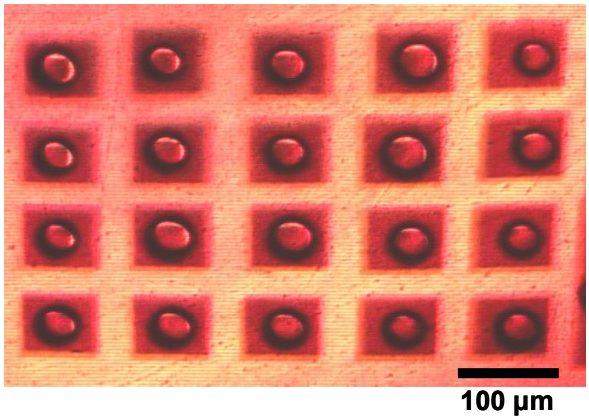

Fig. 8. An array of single particles, formed from multiple single particle square traps. Each particle is individually addressable. [63]

5. CONCLUSION

We have described three examples of MOEMS applications that use MEMS micromirrors. In the first example, a two-axis analog micromirror array is used to expand the capacity of wavelength-selective switches from 1xN to 1xN^2. Experimentally, a 1x32 WSS, the largest WSS to our knowledge, was successfully demonstrated. In the second example, a 2-D scanner with large mirror area and large scan angle was used to implement endoscopic optical coherence tomography. An axial resolution of 5 µm and lateral resolutions of 12 µm were achieved. In the third example, the digital micromirror device (DMD) chip made by Texas Instruments was used to power a novel optoelectronic tweezers for parallel manipulation of microparticles and biological cells. In each of the examples, MEMS provides the key enabling components for the applications. The maturity of MOEMS components will greatly accelerate the insertion of these new technologies in field use.

6. ACKNOWLEDGMENT

The author wishes to thank the members of the Integrated Photonics Lab at UCLA and UC Berkeley and the collaborators for their contributions. Jui-che Tsai, Dr. Li Fan, Chao-hsi Chi, Dr. Dooyoung Hah contributed to the work on wavelength-selective switches. Wibool Piyawattanametha, Dr. Li Fan, Shuting Hsu, Makoto Fujino, and Paul R.

Herz, Aaron D. Aguirre, Yu Chen in Professor James G. Fujimoto's group at MIT contributed to the work on endoscopic optical coherence tomography. Pei Yu Chiou and Aaron Ohta were responsible for the work on optoelectronic tweezers. These projects are supported by DARPA/SPAWAR under #N66001-00-C-8088, National Science Foundation Biophotonics program under #BES-0119494, the Center for Cell Mimetic Space Exploration (CMISE), a NASA University Research, Engineering, and Technology Institute (URETI) under #NCC 2-1364.

REFERENCES

1. Aksyuk, V.A., Pardo, F., Bolle, C.A., Arney, S., Giles, C.R., Bishop, D.J., "Lucent Microstar micromirror array technology for large optical crossconnects," Proceedings of the SPIE, MOEMS and Miniaturized Systems, Sept. 2000, Santa Clara, CA, pp. 320-324.
2. R. Ryf et al., "1296-port MEMS transparent optical crossconnect with 2.07Petabit/s switch capacity," in Proceedings of 2001 OFC postdeadline paper, PD28.
3. D. T. Neilson and R. Ryf, "Scalable micro mechanical optical crossconnects," 2000 IEEE/LEOS Annual Meeting, Paper ME2.
4. Neilson, D.T., et al.,"Fully Provisioned 112x112 Micro-Mechanical Optical Crossconnect With 35.8Tb/s Demonstrated Capacity," Optical Fiber Communication Conference, OFC 2000, March 7-10, Baltimore, MD, Vol. 4, pp.202-204.
5. Lin, L.Y., Goldstein, E.L., "Opportunities and Challenges for MEMS in Lightwave Communications," IEEE J. Sel. Topics Quantum Elec., Vol. 8, No. 1, p.163, 2002.
6. Syms, R.R.A., "Scaling Laws for MEMS Mirror-Rotation Optical Cross Connect Switches," IEEE J. Lightwave Tech., Vol. 20, No. 7, p. 1084, 2002.
7. Y. Mizuno et al., "A 2-axis comb-driven micromirror array for 3D MEMS switches," 2002 IEEE/LEOS International Conference on Optical MEMs, pp. 17 –18, 2002.
8. Sawada, R.; Yamaguchi, J.; Higurashi, E.; Shimizu, A.; Yamamoto, T.; Takeuchi, N.; Uenishi, Y. "Single Si crystal 1024ch MEMS mirror based on terraced electrodes and a high-aspect ratio torsion spring for 3-D cross-connect switch," 2002 IEEE/LEOS International Conference on Optical MEMs, pp. 11 –12, 2002.
9. Aksyuk V.A., Simon, M.E., Pardo, F., Arney S., Lopez, D., and Villanueva, A., "Optical MEMS Design for Telecommunications Applications," 2002 Solid-State Sensor and Actuator Workshop Tech. Digest, June 2-6, Hilton Head, SC, pp.1-6.
10. N. Kouma et al., "A multi-step DRIE process for a 128x128 micromirror array," 2003 IEEE/LEOS International Conference on Optical MEMs, pp. 53 –54, 2003.
11. V. A. Aksyuk et al., "238x238 micromechanical optical cross connect," IEEE Photonics Technol. Lett., Vol. 15, pp.587-9, April 2003.
12. V. A. Aksyuk et al., "Beam-steering micromirrors for large optical cross-connects," IEEE J. Lightwave Tech., Vol. 21, No. 3, p. 634, 2003.
13. Sawada, R.; Yamaguchi, J.; Higurashi, E.; Shimizu, A.; Yamamoto, T.; Takeuchi, N.; Uenishi, Y. "Improved single crystalline mirror actuated electrostatically by terraced electrodes with high aspect-ratio torsion spring," 2003 IEEE/LEOS International Conference on Optical MEMs, pp. 153 –154, 2003.
14. I. Brener et al., "Nonlinear servo control of MEMS mirrors and their performance in a large port-count optical switch," in Proceedings of 2003 OFC, Paper WM1.
15. J. I. Dadap et al., "Modular MEMS-based optical cross-connect with large port-count," IEEE Photonics Technol. Lett., Vol. 15, pp.1773-5, Dec. 2003.
16. C. Pu et al., "Electrostatic actuation of 3-D MEMS mirrors by sidewall electrodes," 2003 IEEE/LEOS International Conference on Optical MEMs, pp. 129 –130, 2003.
17. X. Zheng et al., "Three-dimensional MEMS photonic cross-connect switch design and performance," IEEE J. Sel. Topics Quantum Elec., Vol. 9, No. 2, p.571, 2003.
18. A. Gasparyan, et al., "Drift-free, 1000G mechanical shock tolerant single-crystal silicon two-axis MEMS tilting mirrors in a 1000x1000-port optical crossconnect", in Proceedings of 2003 OFC postdeadline paper, PD36.
19. M. Kozhevnikov et al., "Micromechanical optical crossconnect with 4-f relay imaging optics," IEEE Photonics Technol. Lett., Vol. 16, pp.275-7, Jan. 2004.

20. H. Toshiyoshi and H. Fujita, "Electrostataic Micro Torsion Mirrors for an Optical Switch Matrix," IEEE J. Microelectromechanical Systems, Vol. 5, p. 231, 1996.
21. L.Y. Lin, E.L. Goldstein, and R.W. Tkach, "Free-space micromachined optical switches with submillisecond switching time for large-scale optical crossconnects," IEEE Photonics Technology Letters, vol.10, p.525-7, 1998.
22. B. Hehin, K.Y. Lau, and R.S. Muller, "Magnetically actuated micromirrors for fiber-optic switching," Solid-State Sensors and Actuator Workshop, Hilton Head Island, South Carolina, 1998.
23. R.T. Chen, H. Nguyen, M.C. Wu, "A high-speed low-voltage stress-induced micromachined 2x2 optical switch," IEEE Photonics Technol. Lett., Vol. 11, pp.1396-8, November 1999.
24. L.Y. Lin, E.L. Goldstein, and R.W. Tkach, "Angular-precision enhancement in free-space micromachined optical switches," IEEE Photonics Technology Letters, vol.11, p.1253-5, 1999.
25. L.Y. Lin, E.L. Goldstein, and R.W. Tkach, "Free-space micromachined optical switches for optical networking," IEEE Journal of Selected Topics in Quantum Electronics, Vol. 5, P.4-9, 1999.
26. L.-Y. Lin, E.L. Goldstein, R.W. Tkach, "On the expandability of free-space micromachined optical cross connects," J. Lightwave Technology, Vol. 18, pp. 482 –489, 2000.
27. Li Fan, S. Gloeckner, P. D. Dobblelaere, S. Patra, D. Reiley, C. King, T. Yeh, J. Gritters, S. Gutierrez, Y. Loke, M. Harburn, R. Chen, E. Kruglick, M. Wu and A. Husain, "Digital MEMS switch for planar photonic crossconnects," 2002 Optical Fiber Communication (OFC) Conference, Paper TuO4, Anaheim, California, 2002
28. R. L. Wood, R. Mahadevan, and E. Hill, "MEMS 2-D matrix switch," 2002 Optical Fiber Communication (OFC) Conference, Paper TuO2, Anaheim California, 2002.
29. Y. Yoon, K. Bae, and H. Choi, "An optical switch with newly designed electrostatic actuators for optical cross connects," 2002 IEEE/LEOS International Conference on Optical MEMS, Lugano, Switzerland, 2002.
30. J.E. Ford, V.A. Aksyuk, D.J. Bishop, and J.A. Walker, **"**Wavelength add-drop switching using tilting micromirrors," J. Lightwave Technology, vol. 17, no. 5, pp. 904-11, 1999.
31. D. Hah, S. Huang, H. Nguyen, H. Chang, H. Toshiyoshi, and M. C. Wu, "A low voltage, large scan angle MEMS micromirror array with hidden vertical comb-drive actuators for WDM routers," 2002 Optical Fiber Communication (OFC) Conference, Paper TuO-3, Anaheim, California.
32. D. Hah, S. Huang, H. Nguyen, H. Chang, J. C. Tsai, and M. C. Wu, "Low voltage MEMS analog micromirror arrays with hidden vertical comb-drive actuators," Solid-State Sensor, Actuator, and Microsystems Workshop, June 2002, p.11-14.
33. http://www.sandia.gov/mstc/technologies/micromachines/summit5.html
34. D. M. Marom et al., "Wavelength-selective 1x4 switch for 128 WDM channels at 50 GHz spacing," in Proceedings of 2002 OFC, postdeadline paper, FB7.
35. D. M Marom et al., "Wavelength selective 4×1 switch with high spectral efficiency, 10 dB dynamic equalization range and internal blocking capability," ECOC 2003, Paper Mo3.5.3.
36. D. Lopez, et al., "Monolithic MEMS optical switch with amplified out-of-plane angular motion," Proc. 2002 IEEE/LEOS International Conf. Optical MEMS.
37. D. S. Greywall et al., "Monolithic fringe-field-activated crystalline silicon tilting-mirror devices," J. Microelectromechanical Systems, vol. 12, no. 5, pp.702-707, Oct. 2003.
38. S. Huang, J. C. Tsai, D. Hah, H, Toshiyoshi, and M. C. Wu, "Open-loop operation of MEMS WDM routers with analog micromirror array," in Proceedings of 2002 IEEE/LEOS Optical MEMS Conf., pp.179-180.
39. T. Ducellier, et al., "The MWS 1x4: a high performance wavelength switching building block," in Proceedings of ECOC 2002, session 2.3.1.
40. W. P. Taylor et al., "A high fill factor linear mirror array for a wavelength selective switch," Journal of Micromechanics and Microengineering, 14 (2004) pp.147–152.
41. Jui-che Tsai, Sophia Huang, Dooyoung Hah, and Ming C. Wu, "Wavelength-Selective 1xN^2 Switches with Two-Dimensional Input/Output Fiber Array," Proc. Conference on Lasers and Electro-Optics (CLEO 2003), Baltimore, Maryland, June 1-6, 2003, (Opt. Soc. America, Salem, MA) Paper CTuQ.
42. Jui-che Tsai, Sophia Huang, Dooyoung Hah, and Ming C. Wu, "Analog Micromirror Arrays with Orthogonal Scanning Directions for Wavelength-Selective 1xN^2 Switches," 12th International Conference on Solid-State Sensors and Actuators (Transducers '03), Boston, MA, June 2003.
43. J. C. Tsai, S. Huang, and M. C. Wu, "High fill-factor two-axis analog micromirror array for 1xN2 wavelength-selective switches," Proc. of MEMS 2004, pp. 101-104.
44. J. C. Tsai, L. Fan, D. Hah, and M. C. Wu, "A high fill-factor, large scan-angle, two-axis analog micromirror array driven by leverage mechanism," in Proceedings of 2004 IEEE/LEOS Optical MEMS Conf., pp.30-31.

45. J. C. Tsai, L. Fan, D. Hah, and M. C. Wu, "A high fill-factor, large scan-angle, two-axis analog micromirror array driven by leverage mechanism," in Proceedings of 2004 IEEE/LEOS Optical MEMS Conf., pp.30-31.
46. Tearney, G.J., M.E. Brezinski, B.E. Bouma, S.A. Boppart, C. Pitvis, J.F. Southern, and J.G. Fujimoto, In vivo endoscopic optical biopsy with optical coherence tomography. Science, 1997. 276(5321): p. 2037-9.
47. Dickensheets, D.L. and G.S. Kino, Micromachined scanning confocal optical microscope. Optics Letters, 1996. 21(10): p. 764-766.
48. Piyawattanametha, W., H. Toshiyoshi, L. LaCosse, and M.C. Wu. Surface-micromachined confocal scanning optical microscope. in Conference on Lasers and Electro-Optics (CLEO 2000). Technical Digest. Postconference Edition. TOPS Vol. 39. 2000. San Francisco, CA, USA: Opt. Soc. America.
49. K. Murakami, A. Murata, T. Suga, H. Kitagawa, Y. Kamiya, M. Kubo, K. Matsumoto, H. Miyajima, and M. Katashiro, "a miniature confocal optical microscope with mems gimbal scanner", The 12th International Conference on Solid State Sensors, Actuators and Microsystems, Boston, June 8-12, 2003, pp. 587-590
50. K. Murakami, et. al., "A MEMS gimbal scanner for a miniature confocal microscope", Proc. Optical-MEMS, 2002, TuA2 pp.9-10
51. Pan, Y., H. Xie, and G.K. Fedder, Endoscopic optical coherence tomography based on a microelectromechanical mirror. Optics Letters, 2001. 26(24): p. 1966-8.
52. Zara, J.M., S. Yazdanfar, K.D. Rao, J.A. Izatt, and S.W. Smith, Electrostatic micromachine scanning mirror for optical coherence tomography. Optics letters, 2003. 28(8): p. 628-30.
53. Wibool Piyawattanametha, Li Fan, Shuting Hsu, Makoto Fujino, Ming C. Wu, Paul R. Herz, Aaron D. Aguirre, Yu Chen, James G. Fujimoto, "Two-dimensional endoscopic MEMS scanner for high resolution optical coherence tomography," Proc. Conference of Lasers and Electro-Optics (CLEO), Paper CWS2, San Francisco, California, May 17-21, 2004.
54. W. Piyawattanametha, P. Patterson, D. Hah, H. Toshiyoshi, and M. Wu, "A 2D Scanner by Surface and Bulk Micromachined Angular Vertical Comb Actuators," International Conference on Optical MEMS, August 18-21, Hawaii, USA, pp. 93-94
55. Dooyoung Hah, Patterson PR, Nguyen HD, Toshiyoshi H, Wu MC. "Theory and experiments of angular vertical comb-drive actuators for scanning micromirrors," IEEE Journal of Selected Topics in Quantum Electronics, vol.10, no.3, May-June 2004, pp.505-13.
56. Fujino M, Patterson PR, Nguyen H, Piyawattanametha W, Wu MC. "Monolithically cascaded micromirror pair driven by angular vertical combs for two-axis scanning," IEEE Journal of Selected Topics in Quantum Electronics, vol.10, no.3, May-June 2004, pp.492-7.
57. A. Ashkin, J. M. Dziedzic, J. E. Bjorkholm, and S. Chu, "Observation of a single-beam gradient force optical trap for dielectric particles," Optics Letters, 11(5), pp. 288-290, 1986.
58. H. A. Pohl, Dielectrophoresis. Cambridge: Cambridge University Press, 1978.
59. T. Muller, A. Gerardino, T. Schnelle, S. G. Shirley, F. Bordoni, G. Degasperis, R. Leoni, and G. Fuhr, "Trapping of micrometer and sub-micrometer particles by high-frequency electric fields and hydrodynamic forces," J. Physics D – Applied Physics, 29(2), pp. 340-349, 1996.
60. P. Y. Chiou, Z. Chang, Zehao, and M. C. Wu, "A Novel Optoelectronic Tweezer Using Light Induced Dielectrophoresis," Proc. IEEE/LEOS International Conf. Optical MEMS, pp. 8-9, 2003.
61. P. Y. Chiou, W. Wong, J. C. Liao, and M. C. Wu, "Cell Addressing and Trapping Using Novel Optoelectronic Tweezers," Proc. IEEE MEMS conference, pp. 21-24, 2004.
62. Aaron T. Ohta, Pei Yu Chiou, Ming C. Wu, "Dynamic DMD-driven optoelectronics tweezers for microscopic particle manipulation," Proc. Conference of Lasers and Electro-Optics (CLEO), Paper CWS5, San Francisco, California, May 17-21, 2004.
63. Aaron T. Ohta, Pei-Yu Chiou, and Ming C. Wu, "dynamic array manipulation of microscopic particles via optoelectronic tweezers," Proc. Solid State Sensor, Actuator and Microsystems Workshop (Hilton Head 2004) Hilton Head Island, South Carolina, June 6-10, 2004.
64. D. G. Grier, "A revolution in optical manipulation," Nature, vol. 424, pp. 810-816, 2003.
65. L. J. Hornbeck, "Deformable-Mirror Spatial Light Modulators," Spatial Light Modulators and Applications III, SPIE Critical Reviews, vol. 1150, pp. 86-102, 1989.